Spin-spin and tensor observables in the isovector nucleon-nucleon force

T. Hippchen and J. Speth
Institut für Kernphysik der Kernforschungsanlage, D-5170 Jülich, West Germany

Mikkel B. Johnson
Los Alamos National Laboratory, Los Alamos, New Mexico, 87545
(Received 16 March 1989)

We justify the inclusion of the rho meson in the Bonn potential in terms of the $N\bar{N}\rightarrow\pi\pi$ helicity amplitude analysis. The tensor observables are well reproduced with the resulting interaction. Consequences for the momentum dependence of the spin-longitudinal and spin-transverse effective interactions are discussed.

I. INTRODUCTION

Recently[1] the ability of the Bonn nucleon-nucleon interaction to reproduce the energy dependence of the tensor NN scattering observables has been questioned. At issue is the form of the coupling of the ρ meson to the nucleons. The long-range part of the tensor force is, of course, provided by the one-pion-exchange potential (OPEP). At short distances the OPEP tensor force becomes progressively stronger and must be regulated to avoid unphysical consequences. The ρ meson contributes a tensor force of sign opposite to the pion and effectively plays this role. For this and related reasons the ρ meson is extremely important in the theoretical description of the nucleon-nucleon interaction and has far-ranging consequences, e.g., for the saturation of nuclear matter,[2] pion condensation,[3] Gamow-Teller and magnetic $M1$ transitions,[4] and the isovector spin-isospin response of nuclei.[5]

Because the ρ meson is such an important piece of the nucleon-nucleon interaction, we have undertaken the current investigation to provide a firmer theoretical basis for its inclusion in the Bonn potential. The Bonn potential assumes that the ρ meson is an elementary particle of zero width, whose coupling to nucleons is specified by coupling constants and a form factor $v(q)$ parametrized as

$$v(q)=\frac{\Lambda^2-m_\rho^2}{\Lambda^2+\mathbf{q}^2}\ , \tag{1.1}$$

where $\mathbf{q}$ is the meson momentum, m_ρ is the ρ-meson mass, and Λ is a parameter specifying the cutoff in momentum. The coupling constants and form factor are determined by a fit to the nucleon-nucleon phase shifts.

We know, in fact, that the ρ meson is not a structureless elementary particle and that it is strongly coupled to two pions. The details of how the ρ meson couples to nucleons may be extracted from the pseudophysical $N\bar{N}\rightarrow\pi\pi$ amplitudes[6] having $J=1$ and $I=1$, $f_-^1(t)$. Such an analysis then provides theoretical values for the coupling constant and momentum cutoff directly from theory.

In this paper we begin by finding an expression for the ρ-meson exchange potential in terms of the $N\bar{N}\rightarrow\pi\pi$ helicity amplitude.[7] It is important for our analysis to include the interference terms between the ρ exchange and the $\pi\pi$ continuum, and in addition a cutoff in coordinate space to regulate the short-distance behavior of the potential. Because in our approach the ρ meson is actually a composite object of distributed mass, we have been unable to parametrize the helicity analysis by a simple pole of mass $m_{\rho_1}=770$ MeV, the physical rho-meson mass. However, we have found it sufficient over the limited range of momentum transfer for which the $N\bar{N}\rightarrow\pi\pi$ helicity amplitudes are known to add to this a second piece of a slightly longer range with $m_{\rho_2}=650$ MeV, each with a form factor as given in Eq. (1.1). Using this theoretically determined ρ-meson contribution, the NN phase shifts are refit by adjusting slightly the σ-meson coupling parameters, and the Fermi-liquid parameters are evaluated. We find excellent reproduction of the energy dependence of the tensor observables. The corresponding spin-isospin Fermi-liquid parameter is $g_0'(NN)=0.70$. [We will generally quote g_0' in the "Jülich units" (302 MeV fm^3). The connection to pionic units is $g_0'(\text{pionic})\simeq\frac{3}{4}g_0'(\text{Jülich})$. Sometimes "Stony Brook units" are also used, for which $g_0'(\text{Stony Brook})=2g_0'(\text{Jülich})$.]

II. THE ρ-MESON EXCHANGE

A. Helicity amplitude analysis

We will base our analysis on the results of Ref. 8, which are obtained from the more detailed formalism in Ref. 6. According to this work, the ρ-meson potential is related to the helicity amplitude $f_-^1(t)$ by

$$V_\rho(q)=\tfrac{1}{3}\boldsymbol{\tau}_1\cdot\boldsymbol{\tau}_2 I(q^2)q^2[S_{12}(q)-2q^2\boldsymbol{\sigma}_1\cdot\boldsymbol{\sigma}_2]\ , \tag{2.1}$$

where $S_{12}(q)$ is the tensor operator and

$$I(q^2)=\int_{4\mu^2}^{\infty}\frac{\rho(t)}{t+q^2}dt \tag{2.2a}$$

with

$$\rho(t)=\frac{3(t-4\mu^2)^{3/2}}{32M^2\sqrt{t}}|f^1_-(t)|^2 . \quad (2.2b)$$

Here μ is the pion mass and M the nucleon mass. When equated to the ρ-meson exchange potential in the nonrelativistic limit[9] we find, approximately,

$$I(q^2)=\frac{v^2(q^2)}{q^2+m_\rho^2}\frac{\tilde{f}_\rho^2}{m_\rho^2}=\frac{C_\rho}{m_\pi^2}\frac{1}{q^2+m_\rho^2}v^2(q^2) , \quad (2.3)$$

where the effective ρ-meson nucleon coupling $\tilde{f}_\rho$ is related to the coupling parameters f_ρ and g_ρ of Ref. 9 as

$$\tilde{f}_\rho^2=\left[\frac{m_\rho}{2M}\right]^2 g_\rho^2\left[1+\frac{f_\rho}{g_\rho}\right]^2 \quad (2.4)$$

and $v(q)$ is given by Eq. (1.1). One also sometimes introduces the π-to-ρ coupling constant ($f_\pi^2=1$)

$$C_\rho\equiv\left[\frac{\tilde{f}_\rho m_\pi}{f_\pi m_\rho}\right]^2=\frac{g_\rho^2}{g_\pi^2}\left[1+\frac{f_\rho}{g_\rho}\right]^2 . \quad (2.5)$$

The familiar "strong ρ" coupling is obtained from the Höhler-Pieterinen analysis.[7] For our work we take the helicity amplitudes for the background as given in Ref. 10. Parametrizing these results to within the quoted errors we obtain

$$f^1_-(t)=\frac{-f_0\Gamma}{t-x_0+i\Gamma} \quad (2.6)$$

with $f_0=1.92$, $x_0=29\mu^2$, and $\Gamma=4.8\mu^2$. We then find that

$$C_\rho=2.3$$

and (2.7)

$$m_\rho=5.5\mu$$

give an acceptable parametrization of Eq. (2.2a) over the interval $4\mu^2\le t\le 50\mu^2$, if we take $v(q)=1$. The value in Eq. (2.7) agrees, to within errors, with that obtained in Ref. 7. Including the 2π background, we have

$$\mathrm{Re}f^1_-(t)=\frac{-f_0\Gamma(t-x_0)}{(t-x_0)^2+\Gamma^2}+\frac{A}{t-B} , \quad (2.8)$$

where now $x_0=29$, $\Gamma=4.8$, $A=13$, $B=0.6$ (in units of μ^2), and $f_0=1.92$.

B. Form factors

Before considering the representation of $V_\rho(q)$ including the 2π background, it is necessary to discuss the issue of form factors. The results in Eq. (2.7) correspond to a pointlike coupling $[v(q)=1]$ of the ρ to nucleon. We have found it impossible to find an acceptable fit for any other $v(q)$. This is a source of two problems to which we return. One is that $v(q)$ adds a momentum dependence that is not consistent with the $N\bar{N}\to\pi\pi$ amplitude, and the other is that $v^2(q=0)$ rescales the magnitude of $V_\rho(q)$ so that the *effective* coupling constant is actually

$$C_{\rho,\mathrm{eff}}=v^2(0)C_\rho . \quad (2.9)$$

In Table I we show values of C_ρ and $C_{\rho,\mathrm{eff}}$ corresponding to various Bonn potentials. In order to agree with the helicity analysis given above $C_\rho=2.3$. We see that $C_{\rho,\mathrm{eff}}$ for all of the Bonn interactions falls short of this Höhler-Pieterinen value, corresponding to interactions that are apparently too weak. We note in passing that if one wants to include form factors and a value of C_ρ compatible with *the NN phase shifts,* then this C_ρ will be in most cases substantially *larger* than 2.

The differences noted above are interpreted as follows. The helicity analysis is expected to give the two-body force at sufficiently long range, say $r\gtrsim r_c$. For distances $r<r_c$, poorly known effects, such as the explicit participation of quarks and gluons, begin to play a role. To retain $V_\rho(r)$ down to distances $r<r_c$ would be practical only if the other contributions were known and also included in the potential. Since this is not the case, we are entitled to modify $V_\rho(r)$ at these distances to simulate the omitted contributions. Consequently, we cut off $V_\rho(r)$ at some small distance, which can be conveniently accomplished by multiplying $V_\rho(r)$ by a function $f(r)$

$$\tilde{V}_\rho(r)=V_\rho(r)f(r) . \quad (2.10)$$

The function $\tilde{V}_\rho(r)$ is thus the potential that we will use in the one-boson-exchange (OBE) part of the potential. A convenient function $f(r)$ is the one given by

$$f(r)=1-j_0(r/r_c) , \quad (2.11)$$

where j_0 is a spherical Bessel function. This approaches $\frac{1}{2}$ for $r/r_c\simeq 1.895$, unity for $r=\pi r_c$, and for $r>\pi r_c$, $f(r)$ has damped oscillations about unity with period $2\pi r_c$. These oscillations are a small effect, and they have no significant consequences for our work.

About the only theoretical guidance available in choosing r_c is that $f(r)$ should approach unity for internucleon spacings of about 1 fm, implying that $r_c\lesssim\pi^{-1}\simeq 0.3$ fm (or $q_c\gtrsim 650$ MeV/c). In practice the final choice of r_c may have to be determined by fitting the nucleon-nucleon phase shifts. The function $f(r)$ in Eq. (2.11) has the valuable property that its Fourier transform is the sum of two delta functions ($q_c=\hbar c/r_c$)

$$f(q)=(2\pi)^3\delta(\mathbf{q})-2\pi^2\frac{\delta(q-q_c)}{q^2} , \quad (2.12)$$

TABLE I. Values of C_ρ in various Bonn potentials including the effect of the form factor at $q=0$.

Source	$C_{\rho,\mathrm{eff}}$	C_ρ
OBEPT[a]	1.75	3.23
OBEPQ[a]	1.49	2.83
HEA[b]	1.31	2.11
Full[a]	1.43	2.94
Höhler-Pieterinen	2.3	2.3

[a]Reference 9.
[b]Reference 11.

which makes the function $\tilde{V}_\rho(r) \equiv V_\rho(r) f(r)$ easy to express in momentum space using the approximation techniques of Ref. 12. In that paper it is shown that if

$$V_\rho(q) = \tau_1 \cdot \tau_2 I(q^2)(\sigma_1 \cdot \mathbf{q} \sigma_2 \cdot \mathbf{q} - q^2 \sigma_1 \cdot \sigma_2) , \qquad (2.13)$$

then

$$\tilde{V}_\rho(q) = (\sigma_1 \cdot \mathbf{q} \sigma_2 \cdot \mathbf{q} - q^2 \sigma_1 \cdot \sigma_2) \times [I(q^2) - I(q^2 + q_c^2)] \tau_1 \cdot \tau_2 + \Delta V_\rho(q) , \qquad (2.14)$$

where

$$\Delta V_\rho(q) = \tfrac{2}{3} \sigma_1 \cdot \sigma_2 q_c^2 I(q^2 + q_c^2) \tau_1 \cdot \tau_2 . \qquad (2.15)$$

In the case that the ρ meson is given by Eq. (2.3), we have

$$\tilde{I}(q^2) \equiv I(q^2) - I(q^2 + q_c^2) = \frac{\tilde{f}_\rho^2}{m_\rho^2} \frac{q_c^2}{(q^2 + m_\rho^2)(q^2 + q_c^2 + m_\rho^2)} . \qquad (2.16)$$

We see that Eq. (2.16) now has the same form as Eq. (2.3) with

$$v^2(q) = \frac{q_c^2}{q^2 + q_c^2 + m_\rho^2} . \qquad (2.17)$$

In other words, *a short-distance cutoff in coordinate space is equivalent to imposing a form factor.* Note that, as in the Bonn potential, $v^2(0) \neq 1$ in Eq. (2.17). If $q_c \cong 1$ GeV/c ($r_c \simeq 0.2$ fm), then we understand the differences between the values in Table I and the value $C_\rho = 2.3$ in Eq. (2.7). A similar cutoff procedure was applied in the Paris potential.[13] In Fig. 1 we compare this helicity analysis with the Paris momentum space potential [$V_\rho(q)$] for Paris is determined from the isovector tensor force[14] with the OPEP subtracted and various Bonn potentials. In all cases, the realistic interactions fall below the helicity analysis, as we would expect to occur if one uses a cutoff in coordinate space.

Finally, we note in Eq. (2.14) that our cutoff procedure introduces an extra short-range, spin-dependent force. For $q_c \simeq 1$ GeV/c, this piece could be simulated by an exchanged meson of mass about 2 GeV. Thus, $\Delta V_\rho(r)$ contributes dominantly at distances less than r_c. As the size of $\Delta V_\rho(r)$ is obviously sensitive to the details of the shape of the function $f(r)$, we have dropped this term in our numerical results shown below. Dropping $\Delta V_\rho(r)$ is consistent with our philosophy that the potential cannot be determined theoretically for $r < r_c$ at the present time.

C. Helicity analysis including 2π continuum

We note that when Eq. (2.8) is used for Re$f_-^1(t)$ the resulting potential $V_\rho(q)$ contains the 2π continuum, the ρ meson, and a $\rho-\pi\pi$ interference term that corresponds to the virtual decay of the ρ meson as it is exchanged. The corresponding $V_\rho(q)$ calculated from Eqs. (2.1) and (2.2) is *not* appropriate as an *NN* potential to be used in a Schrödinger equation because the 2π continuum is largely contained in the iterated OPEP. To make an appropriate potential we must subtract this part out of $V_\rho(q)$. (The full subtraction of the empirical continuum may be too severe for the OBEP because the crossed box and 2π with Δ intermediate states contribute to the continuum. We believe that these are small, but in any case they are added back into the full Bonn potential.) We show in Fig. 2 $V_\rho(q)$ calculated with the 2π continuum and with the 2π continuum subtracted. These are compared to the ρ meson (solid line in Fig. 1). The difference between the dashed and solid curves is the $\rho-\pi\pi$ interference term that arises when Eq. (2.8) is squared. This piece is not contained explicitly in the Bonn potential, either in OBEP or in the full model, and we therefore want to include it as part of our $V_\rho(r)$. We have found that this case, $\rho+(\rho-\pi\pi)$ interference, can be well represented by a two-component ρ meson of the form

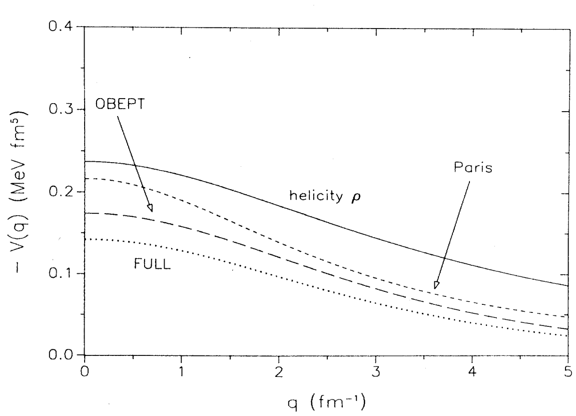

FIG. 1. The rho-meson interaction $V(q) = [(\hbar c)^5/(2\pi)^3]\tilde{I}(q)$ for various models. Helicity, ρ meson only (solid); Paris (short-dashed); Bonn OBEPT (long-dashed); and full Bonn (dotted).

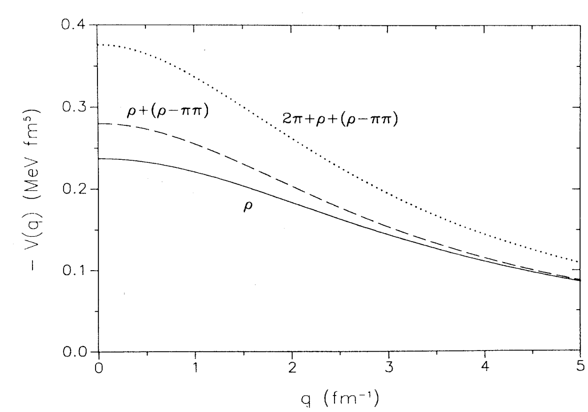

FIG. 2. The rho-meson interaction $V(q) = [(\hbar c)^5/(2\pi)^3]\tilde{I}(q)$ determined from the helicity analysis. Full helicity interaction (dotted); with 2π continuum subtracted (dashed); and with 2π continuum and $\rho - 2\pi$ interference subtracted (solid).

TABLE II. Various parametrizations of the helicity amplitude analysis.

Case	Λ (MeV)	m_{ρ_1} (MeV)	C_{ρ_1}	m_{ρ_2} (MeV)	C_{ρ_2}	r_c
(1) Rho-meson pole only	∞	770	2.3			
(2) Pole+interference	1500	770	2.56	625	0.61	0.19

$$m_\pi^2 \tilde{I}(q) = \left[\frac{\Lambda^2 - m_1^2}{\Lambda^2+q^2}\right]^2 \frac{c_1}{q^2+m_1^2} + \left[\frac{\Lambda^2 - m_2^2}{\Lambda^2+q^2}\right]^2 \frac{c_2}{q^2+m_2^2} \quad (2.18)$$

with the parameters given in Table II. We have imposed a cutoff with $r_c = 0.19$ fm to approximately simulate the cutoff applied to the Paris potential and one sees in Fig. 3 that the results are very similar. It is also clear in Fig. 3 that our helicity potential, the Paris potential, and the full Bonn potential all fall off faster in momentum space and therefore have a larger range in coordinate space then the pure ρ potential (solid curve). The reason for this is that the $\rho-\pi\pi$ interference increases the range.

III. CALCULATIONS

In this section we will use the results of Sec. II to obtain a new one-boson-exchange potential. We saw there that our ρ-meson interaction is considerably stronger than the ones used in the Bonn OBEP interactions and has a range that has been fixed theoretically by the coupling of the ρ meson to the 2π continuum. We want to see whether this makes any difference in the ability of the theory to fit the nucleon-nucleon scattering data.

After refitting the OBEP to the *NN* phase shifts, we will examine the nuclear matter results, specifically the Fermi-liquid parameters, and the effective interactions in the spin-longitudinal and spin-transverse channels.

A. Fit to *NN* phase shifts

We begin with the energy-dependent one-boson-exchange (OBEPT) *NN* potential.[9] This contains two scalar mesons, an isoscalar (with different parameters in $T=0$ and $T=1$ states) and an isovector (δ), the vector mesons ω and ρ, and the pseudoscalar mesons π and η. Their masses and coupling constants as determined in the original work are given in Table III.

To incorporate our helicity analysis, we have given the ρ meson two components in line with Table II, case 2. We then refit the coupling constants of the σ_0, σ_1, and δ and the form factor of the π meson to reproduce the *NN* phase shifts. The new helicity-analysis-based one-boson-exchange potential (OBEPH) incorporates the values for the ρ determined from the helicity analysis. These values are given in Table III. The level of quality of the fit is as good as that of OBEPT. The deuteron properties come out well in both cases. We do not show the phase-shift fit to the data for our new potential because it is quite similar to the old one.

We have also tried fits with different values of r_c. We have found it difficult to find fits to the nucleon-nucleon phase shifts with smaller values of r_c, corresponding to a weaker tensor and strong spin-spin force. For stronger spin-spin forces we generally find improved fits to the $^1P_1$ phase shift, but at the same time the $^3P_2$ phase shift deteriorates considerably. The smaller r_c also weakens

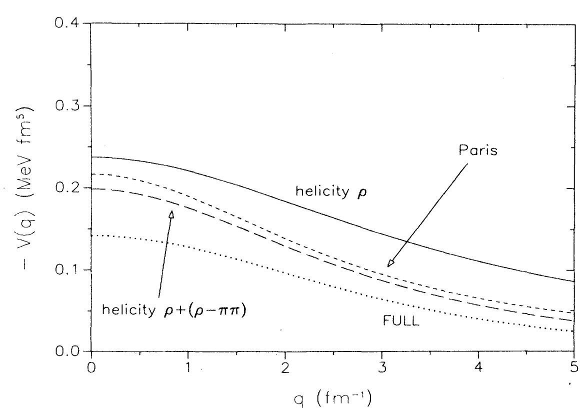

FIG. 3. The rho-meson interaction $V(q) = [(\hbar c)^5/(2\pi)^3]\tilde{I}(q)$ for various models. Helicity with ρ only and $r_c = 0$ (solid); Paris (short-dashed); helicity with $\rho+(\rho-2\pi)$ interference and $r_c = 0.19$ fm (long-dashed); ρ exchange of full Bonn potential (dotted).

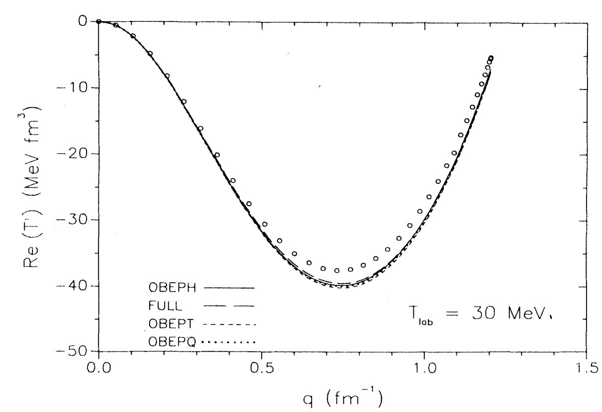

FIG. 4. Theoretical tensor nucleon-nucleon scattering observable compared to experiment (open circles) at laboratory energy of 30 MeV. The theoretical result obtained in this paper, OBEPH, is the solid curve. Also shown are the full Bonn potential (long-dashed), the Bonn OBEPT (short-dashed), and the Bonn OBEPQ (dotted).

TABLE III. Mesons and meson-nucleon interactions. Top, mesons that are the same in the original OBEPT and the new fit. Bottom, mesons whose couplings to nucleons have changed.

	η	ω
$g^2/4\pi$	5.0	20.0
f/g		0.0
m (MeV)	548.8	782.6
Λ (MeV)	1500	1500

	π	σ_0	σ_1	δ	ρ_1	ρ_2
OBEPT						
$g^2/4\pi$	14.6	11.7027	8.8543	1.1585	0.920	
f/g					6.1	
m (MeV)	138.03	615	550	983	769	
Λ (MeV)	1750	2000	2000	2000	1500	
OBEPH						
$g^2/4\pi$	14.6	11.3213	8.7993	1.1465	0.7385	0.1738
f/g					6.1	6.1
m (MeV)	138.03	615	550	983	770	625
Λ (MeV)	2000	2000	2000	2000	1500	1500

the net tensor force to an extent that cannot be repaired by adjustments in the coupling constants of the other mesons.

Next, let us turn to the tensor observables. Love[15] has deduced the energy dependence of the isovector tensor observables from the SM84 *NN* amplitude of Arndt and Roper.[16] These tensor observables are defined in Ref. 17. He has found these at $T_{\rm lab}=30$, 50, 100, 140, and 210 MeV, which we show in Figs. 4–8 compared with the predictions of the energy-independent one-boson-exchange Bonn potential OBEPQ,[9] OBEPT, the full Bonn potential, and our new model, OBEPH. We see that our OBEPH is comparable to the other one-boson-exchange interactions. All of these interactions agree quite well with the data, but the full Bonn potential seems to do somewhat better than the others, especially at the higher energies. The older Holinde, Erkelenz, and Alzetta (HEA) potential[11] was found by Nakayama[18,19] to be inconsistent with the tensor observables; we have confirmed this disagreement but stress that the more recent interactions including our own do not suffer from the difficulties of Ref. 1.

We have therefore not only arrived at an understanding of the strength and range of the ρ-meson contribution to the *NN* interaction based on the helicity analysis, we have shown that the interaction determined in this fashion is consistent with the tensor observables in the *NN* data. Our analysis favors a somewhat stronger ρ-meson coupling than is found in the published Bonn interactions, but the effect of this on the isovector tensor observables is compensated by adjustments in the coupling constants of the scalar mesons.

B. Nuclear matter properties

The low-lying properties of nuclei are determined by the Landau Fermi-liquid parameters.[20] These are ob-

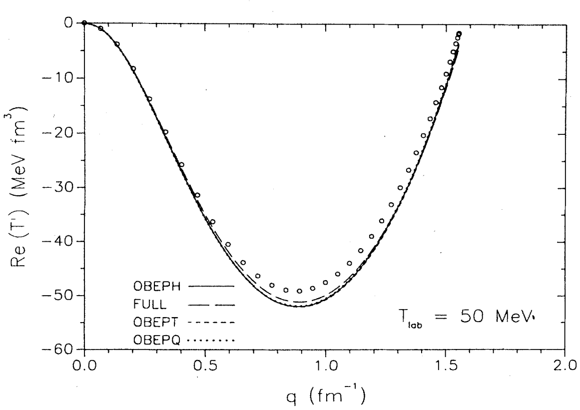

FIG. 5. Theoretical tensor nucleon-nucleon scattering observable compared to experiment at laboratory energy of 50 MeV. The legend is the same as that in Fig. 4.

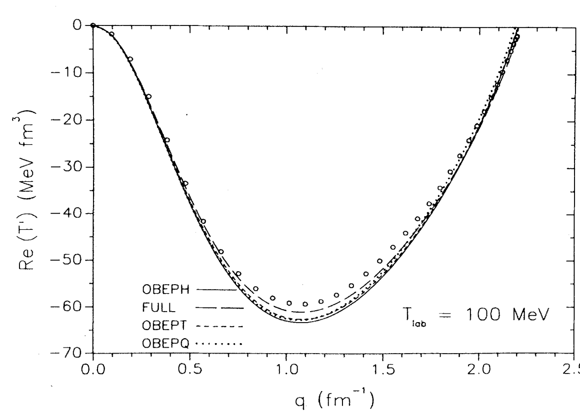

FIG. 6. Theoretical tensor nucleon-nucleon scattering observable compared to experiment at laboratory energy of 100 MeV. The legend is the same as that in Fig. 4.

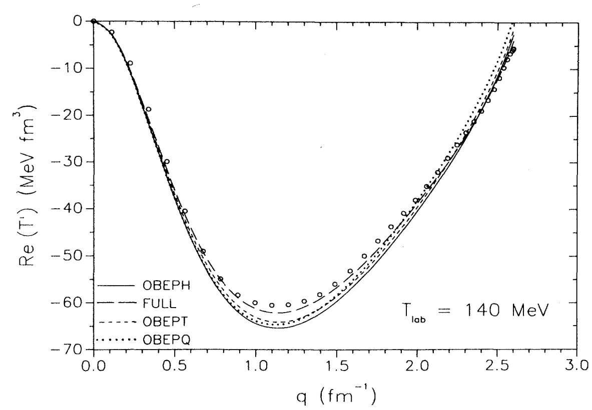

FIG. 7. Theoretical tensor nucleon-nucleon scattering observable compared to experiment at laboratory energy of 140 MeV. The legend is the same as that in Fig. 4.

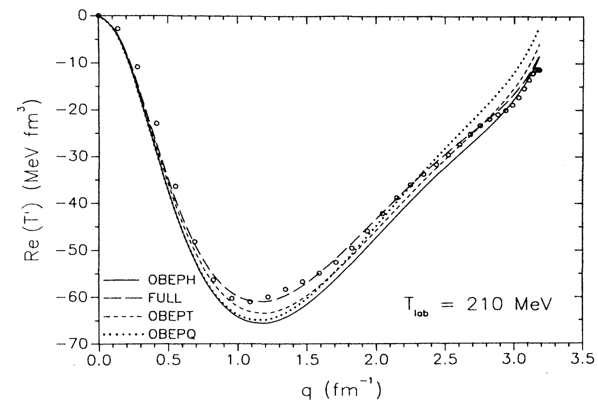

FIG. 8. Theoretical tensor nucleon-nucleon scattering observable compared to experiment at laboratory energy of 210 MeV. The legend is the same as that in Fig. 4.

tained from a G-matrix calculation by taking functional derivative energy density of nuclear matter with respect to the neutron and proton densities. The Landau parameters for the original OBEPT and new OBEPH interactions are given in Table IV. The changes in all the parameters are quite small. The binding energy per particle and the saturation density are nearly the same in the two cases when calculated with a self-consistent effective mass. These values are in good agreement with the empirical values[2] $k_F=1.36$ fm^{-1} and $BE/A=15.68$ MeV.

Of particular interest to us is the Fermi-liquid parameter g_0', because this is directly influenced by the ρ meson. This plays an important role in pion condensation, Gamow-Teller resonances, magnetic $M1$ transitions, and in the isovector spin-isospin response of nuclei. Empirical studies of Gamow-Teller resonances and magnetic $M1$ transitions give[21] values of $g_0'\simeq 0.84$ which fall somewhat short of the values in Table IV. We have tried fitting the NN scattering data with rho mesons of various strengths and find that when the other coupling constants are adjusted to fit the data, g_0' stays very close to its value of $g_0'\sim 0.7$. To pull g_0' substantially away from 0.7, great compromises on the quality of the fit to the data must be made. We have concluded therefore that the value of $g_0'\sim 0.7$ is rather well fixed by the data and presume that the remaining discrepancy with the empirical value is to be remedied by the nuclear matter theory.

Finally, let us remark on the effective isovector interactions in the spin-longitudinal and spin-transverse channels. These may be deduced from the π- and ρ-meson exchange interactions and have the following familiar forms (for energy transfer $\omega=0$):

$$V_L(q)=\frac{f_\pi^2}{m_\pi^2}\sigma_1\cdot\hat{q}\sigma_2\cdot\hat{q}\left[\frac{v_\pi^2(q)q^2}{-q^2-\mu^2}+g_0'\right], \quad (3.1)$$

$$V_T(q)=\frac{f_\pi^2}{m_\pi^2}\sigma_1\times\hat{q}\sigma_2\times\hat{q}\left[\frac{v_\rho^2(q)C_\rho q^2}{-q^2-m_\rho^2}+g_0'\right], \quad (3.2)$$

where g_0' is the familiar Fermi-liquid parameter (Table IV) and C_ρ is the quantity defined in Eq. (2.3). In deriving Eqs. (3.1) and (3.2), it is assumed that the isovector tensor force is not influenced by medium modifications but that the isovector spin-spin force is, leading to the final value of g_0'. Considering short-range correlations and antisymmetry, g_0' picks up contributions from the pion, the ρ meson, and other mesons as well. Nakayama[18] has shown that this particular treatment of the tensor force is reasonably accurate, at least for densities $\rho/\rho_0 \gtrsim \frac{1}{3}$ and $q \lesssim 2$ fm^{-1}.

So we see that our modifications will have some influence on the spin-transverse channel, leading to an increase in C_ρ (see, e.g., Fig. 3) and therefore to a slightly diminished hardening of the spin-transverse response function, which can be measured in electron scattering. Because g_0' is unchanged, the spin-longitudinal response function is also unchanged. These considerations were discussed earlier in Ref. 5.

We finally comment on attempts that have been made

TABLE IV. Landau Fermi-liquid parameters.

Parameter	f_0	f_0'	g_0	g_0'	k_F (fm^{-1})	BE/A (MeV)
Old	−0.91	+0.46	+0.18	+0.69	1.35	14.7
New	−0.95	+0.48	+0.19	+0.71	1.30	13.1

to obtain g_0' directly from the helicity analysis without refitting of the NN phase shifts. Some of these calculations (e.g., Ref. 22) omit the 2π continuum, but others (e.g., Refs. 23–25) include the 2π continuum and its interference with the ρ meson. In all these calculations g_0' was found to be large and we have confirmed the results. For example, in Ref. 22, $g_0'=1.15$. Unfortunately, when the full interaction is included and refit to the NN phases as we do here, the large g_0' is found to be spurious. We believe that the value should be close to $g_0'=0.7$.

IV. SUMMARY AND CONCLUSIONS

We have found that the helicity analysis justifies the inclusion of the ρ meson in the NN potential. The ρ meson found by such a procedure is an effective one whose range in coordinate space is increased by the coupling to the 2π continuum. Including a cutoff for distances $r \lesssim 0.6$ fm to account for nucleon size, the resulting potential fits the NN scattering data. In order to obtain this fit, it is necessary to readjust the coupling constants and form factors of the remaining mesons. The long-range tail survives this procedure. This tail has important consequences for nuclear-matter calculations because the tail is much less cut down by the short-range correlations. However, the value of the Landau parameter g_0' is not altered. This is similar to the results in Ref. 26, where it was found that whereas the A_1 meson changes the potential, the Landau parameters are unchanged once the potential is made to fit the NN scattering data. The tensor observables are in excellent agreement with the NN scattering data, and the concerns expressed in Ref. 1 are thereby satisfied.

ACKNOWLEDGMENTS

The authors express special thanks to G. E. Brown for his motivating influence on this work. We thank J. Haidenbauer for providing the values of the Paris potential, K. Holinde, R. Machleidt, and K. Nakayama for clarifying discussions, and G. Love for providing us with the experimental tensor observables. M. B. Johnson acknowledges the support of the Alexander Von Humboldt Foundation and the U.S. Department of Energy.

[1]G. E. Brown, Prog. Theor. Phys. Suppl. **91**, 92 (1987).
[2]H. A. Bethe, Annu. Rev. Nucl. Sci. **21**, 93 (1971).
[3]W. Weise and G. E. Brown, Phys. Lett. **48B**, 297 (1974).
[4]J. Speth *et al.*, Nucl. Phys. **A343**, 382 (1980); K. Nakayama, S. Krewald, J. Speth, and G. E. Brown, Phys. Rev. Lett. **52**, 500 (1984).
[5]W. M. Alberico, M. Ericson, and A. Molinari, Nucl. Phys. **A379**, 429 (1982).
[6]M. Chemtob, J. W. Durso, and D. O. Riska, Nucl. Phys. **B38**, 141 (1972).
[7]G. Höhler and E. Pieterinen, Nucl. Phys. **B95**, 210 (1975).
[8]M. Brack, D. O. Riska, and W. Weise, Nucl. Phys. **A287**, 425 (1977).
[9]R. Machleidt, K. Holinde, and Ch. Elster, Phys. Rep. **149**, 1 (1987).
[10]J. W. Durso, A. D. Jackson, and B. J. Verwest, Nucl. Phys. **A345**, 471 (1980).
[11]K. Holinde, K. Erkelenz, and R. Alzetta, Nucl. Phys. **A194**, 161 (1972).
[12]E. Oset and W. Weise, Nucl. Phys. **A319**, 477 (1979).
[13]W. N. Cottingham *et al.*, Phys. Rev. D **8**, 800 (1973).
[14]M. Lacombe *et al.*, Phys. Rev. C **21**, 861 (1980).
[15]G. Love (private communication). The experimental points are obtained from the SM84 nucleon-nucleon amplitudes of Arndt and Roper, Ref. 16.
[16]R. A. Arndt and L. D. Roper, Virginia Polytechnic Institute Scattering Analysis Interactive Dial-In Program, Solution SM84.
[17]K. Nakayama, S. Krewald, J. Speth, and G. Love, Nucl. Phys. **A341**, 419 (1984).
[18]K. Nakayama, Ph.D. thesis, University of Bonn, 1985.
[19]K. Nakayama, S. Krewald, J. Speth, and G. Love, Phys. Rev. **C31**, 2307 (1985).
[20]A. B. Midgal, *Theory of Finite Fermi Systems and Applications to Atomic Nuclei* (Wiley, New York, 1967).
[21]J. Speth *et al.*, Nucl. Phys. **A343**, 382 (1980); K. Nakayama, S. Krewald, J. Speth, and G. E. Brown, Phys. Rev. Lett. **52**, 500 (1984).
[22]G. E. Brown, E. Osnes, and M. Rho, Phys. Lett. **163B**, 41 (1985).
[23]M. R. Anastasio and G. E. Brown, Nucl. Phys. **A285**, 516 (1977).
[24]H. Toki and W. Weise, Phys. Lett. **92B**, 265 (1980).
[25]K. Shimizu and A. Faessler, Nucl. Phys. **A333**, 495 (1980).
[26]Th. Hippchen, K. Holinde, and J. Speth, Phys. Lett. B **179**, 192 (1986).